

Mesenchymal stem cell transplantation alleviates Sjögren's syndrome symptoms by modulating Tim-3 expression

Tian Sun^a, Shanshan Liu^a, Guangxia Yang^b, Rujie Zhu^c, Zutong Li^a, Genhong Yao^a,
Hongwei Chen^{a,*}, Lingyun Sun^{a,*}

^a Department of Rheumatology and Immunology, The Affiliated Drum Tower Hospital of Nanjing University Medical School, 321 Zhongshan Road, Nanjing 210008, Jiangsu, China

^b Nanjing Drum Tower Hospital, Clinical College of Traditional Chinese and Western Medicine, Nanjing University of Chinese Medicine, China

^c Department of Rheumatology and Immunology, Nanjing Drum Tower Hospital Clinical College of Nanjing Medical University, China

ARTICLE INFO

Keywords:

MSC transplantation
Sjögren's syndrome
Tim-3
Autoimmune diseases

ABSTRACT

Mesenchymal stem cell (MSC) transplantation has been proven to be an effective treatment for Sjögren's syndrome (SS) to improve salivary gland pathology and exocrine function, but the mechanism remains unclear. A recently reported inhibitory receptor, Tim-3, also appears to be closely related to autoimmune diseases. Here, we aimed to explore the roles of Tim-3 in the pathogenesis of SS and MSC treatment. The results showed that Tim-3 was downregulated in T cells of SS patients and nonobese diabetic (NOD) mice, which is correlated with SS pathogenesis. MSC transplantation ameliorated SS-like symptoms and pathological changes in the submandibular glands with modulated Tim-3 expression, resulting in attenuation of localized inflammation, fibrosis, and epithelial-mesenchymal transition. Furthermore, Tim-3 is crucial for the inhibitory effect of MSCs on PBMC proliferation *in vitro*. Therefore, our work has demonstrated that MSC transplantation effectively mitigates the pathological changes of SS by regulating Tim-3 expression, which provides a novel mechanism of MSC treatment and indicates a brand-new perspective of the combination of inhibitory-receptor-targeted treatment and MSC therapy in SS.

1. Introduction

Sjögren's syndrome (SS) is a systemic autoimmune disease characterized by progressive sicca symptoms, lymphocytic infiltration to exocrine glands, the presence of autoantibodies, systemic involvement, and an increased risk of lymphoma [1]. Primary SS (pSS) does not combine with another systemic autoimmune disease, while complications in secondary SS include rheumatoid arthritis (RA), systemic lupus erythematosus (SLE), or systemic sclerosis. The incidence rate of primary SS was 6.92 (95 % CI 4.98 to 8.86) per 10,000 person-years, and the female/male ratio was 9.15 (95 % CI 3.35 to 13.18). Meanwhile, the prevalence rate in the total population was 60.82 (95 % CI 43.69 to 77.94) cases per 100,000 inhabitants, and the female/male ratio in the prevalence data was 10.72 (95 % CI 7.35 to 15.62) [2]. Similar to other autoimmune diseases, the pathogenesis of SS is complicated and still not well understood. The pathogenesis of SS includes the excessive proliferation of T-helper 1 (Th1) cells and sustained B-cell activation, the progression of organ damage, and the dysfunction of epithelial cells

caused by the inflammatory microenvironment [3,4]. Clinically, although glucocorticoids combined with synthetic disease-modifying antirheumatic drugs were used for SS treatment, the function of the exocrine gland fails to be restored in patients, which requires the development of immunosuppressive therapies for SS treatment.

Mesenchymal stem/stromal cells (MSCs) affect the proliferation and function of immune cells [5] and the differentiation and function of autologous myeloid-derived suppressor cells [6]. Therefore, MSCs have been extensively used to treat graft versus host disease, musculoskeletal tissue damage, autoimmune diseases, chronic degenerative diseases, genetic diseases, and infectious diseases in the clinic [7]. MSC transplantation has also been proven to be an effective treatment for SS. After transplantation into nonobese diabetic (NOD) mice, a well-established SS animal model, MSCs facilitated the increase in salivary flow rate and expression of anti-inflammatory cytokines, simultaneously attenuating salivary gland lymphocyte infiltration and inflammatory cytokines [8]. MSC treatment substantially increased the salivary flow rate, ameliorated disease symptoms, and inhibited inflammatory responses in

* Corresponding authors.

E-mail addresses: chenhw@nju.edu.cn (H. Chen), lingyunsun@nju.edu.cn (L. Sun).

<https://doi.org/10.1016/j.intimp.2022.109152>

Received 3 March 2022; Received in revised form 17 July 2022; Accepted 18 July 2022

Available online 22 August 2022

1567-5769/© 2022 Elsevier B.V. All rights reserved.

SS patients [9]. However, the mechanism of MSC transplantation in treating SS has not been fully revealed.

Coinhibitory receptors (CIRs), also known as immune checkpoints, have attracted much attention because of their indispensable roles in tumor immunotherapies. Immune-related adverse events associated with CIR inhibitors have led to studies on these coinhibitory pathways of immunocytes in autoimmune disease [10,11]. Several biological agents targeting these CIRs recommended in ACR guidelines represent the future direction of the treatment for SS, such as tacrolimus and abatacept with cytotoxic T-lymphocyte-associated antigen-4 (CTLA-4) antibodies [12]. As a critical CIR, the T-cell immunoglobulin (Ig) mucin family containing molecule 3 (Tim-3) is expressed on the surface of both adaptive and innate immune cells [13]. By binding galectin-9 (Gal-9, also called LGALS9) [14], Tim-3 is involved in the pathogenesis of autoimmune diseases, such as SLE [15], RA [16], autoimmune hepatitis [17], and immunoglobulin G4-related disease [18]. Furthermore, Tim-3 has been found to promote tumor cell metastasis by inducing epithelial-mesenchymal transition (EMT), which is also responsible for the dysfunction of exocrine gland epithelial cells in SS [19,20]. Additionally, MSCs secrete Gal-9, a Tim-3 ligand, especially under IFN- γ stimulation [21]. Therefore, we speculated that MSCs may achieve SS treatment via the Gal-9/Tim-3 pathway. Herein, we have expounded on the role of Tim-3 dysfunction in autoimmune activation and lymphocyte infiltration in the pathogenesis of SS in both patients and NOD mice. Moreover, we established the relationship between Tim-3 and MSC transplantation and characterized MSC transplantation-promoted cellular processes in SS, including the inhibition of immune cell proliferation, reduction of immune inflammation in the submandibular gland (SMG), reversal of EMT, and improvement of exocrine functions. Therefore, our study represents the first attempt to explore the mystery of MSC treatment of SS based on Tim-3.

2. Materials and methods

2.1. Patients and healthy controls

All peripheral blood samples were collected from inpatients with primary Sjögren's syndrome in the Department of Rheumatology and Immunology, Affiliated Drum Tower Hospital, Medical School of Nanjing University. The 2002 American-European Consensus Group criteria for Sjögren's syndrome were utilized as the diagnostic criteria, and other autoimmune diseases were excluded. The European League Against Rheumatism (EULAR) Sjögren's Syndrome Disease Activity Index (ESSDAI) score was assessed by experienced clinicians based on clinical manifestations and comprehensive examination results, including antinuclear antibody (ANA) and labial salivary gland biopsy (LSGB). Age- and sex-matched healthy controls were recruited from the Medical Examination Center of the Affiliated Drum Tower Hospital, Medical School of Nanjing University. All research complied with the Declaration of Helsinki. The study was approved by the Ethics Committee of the Affiliated Drum Tower Hospital, Medical School of Nanjing University. All patients and healthy volunteers were informed and consented to this study. Detailed clinical characteristics are described in Table 1.

2.2. Mice

NOD mice are widely described as an experimental model of Sjögren's syndrome based on lymphocytic focal infiltration in the submandibular gland [22]. NOD/ShiLtJGpt mice (female, 6–8 weeks old) and Institute of Cancer Research (ICR) mice (female, 6–8 weeks old) as a wild-type control mouse model [23] were purchased from Gem-Pharmatech Co. Ltd. (Nanjing, China). All mice were bred under specific-pathogen-free conditions in the animal facility of the Affiliated Drum Tower Hospital, Medical School of Nanjing University. All animal experiments followed the institutional guidelines of the Affiliated Drum Tower Hospital of Medical School of Nanjing University and were

Table 1

Clinical characteristics and medications for the SS patients.

Patient	Age/ sex	Disease duration (months)	ESSDAI	LSGB	ANA	Medication
1	55/F	15	8	4	anti-SSA+, anti-SSB+	HCQ
2	62/F	18	6	3	anti-SSA-, anti-SSB-	HCQ
3	27/F	61	8	3	anti-SSA+, anti-SSB-	HCQ, Iguratimod
4	52/F	40	11	4	anti-SSA+, anti-SSB-	Pred, HCQ, MMF
5	44/ M	2	8	4	anti-SSA+, anti-SSB+	Pred, Tacrolimus
6	32/F	8	9	4	anti-SSA+, anti-SSB+	Pred, HCQ
7	36/F	25	4	4	anti-SSA+, anti-SSB-	HCQ
8	27/F	1	7	2	anti-SSA+, anti-SSB+	Pred, HCQ

ESSDAI, EULAR Sjögren's Syndrome Disease Activity Index; LSGB, labial salivary gland biopsy; ANA, antinuclear antibody; Pred, prednisone; HCQ, hydroxychloroquine; MMF, Mycophenolate mofetil.

approved by the Committee of Experimental Animal Administration of the Affiliated Drum Tower Hospital of Medical School of Nanjing University (Approval number: 2020AE01078). At the age of 13 weeks, NOD mice were randomized into two groups. Group 1: NOD mice with caudal vein injection of human umbilical cord-derived MSCs (n = 6), Group 2: NOD mice with caudal vein injection of PBS (n = 6).

2.3. Saliva flow rate

The secretory function of the salivary glands (salivary flow rate, SFR) was determined every 2 weeks from the age of 9 weeks. The body weight of each mouse was recorded before each test. Mild gas anesthesia was induced and maintained during the test with 5 % isoflurane (RWD, R510-22). Stimulation was performed with an intraperitoneal injection of pilocarpine hydrochloride (MCE, HY-B0726) at a dose of 5 mg/kg body weight. [24] A 1.5 ml Eppendorf tube with a piece of cotton wool was prepared and preweighed. For each mouse, a piece of cotton wool was removed from the tube and placed into the mouse's oral cavity for 10 min. Then, the cotton wool piece filled with saliva was removed back into the original tubes and weighed. The saliva flow rate was obtained by calculating the difference between the total weight of the tube and cotton before and after the experiment and then dividing it by 10 min and the weight of the mice. The amount of saliva collected was determined by the gravimetric method. The d-value of SFR before (13 weeks old) and after (15 weeks old) treatment was calculated as Δ SFR.

2.4. Culture and transplantation of MSCs

Human umbilical cord-derived MSCs (UC-MSCs) were acquired from the Stem Cell Center of Jiangsu Province. The details of isolation, purification, and identification were described previously [25]. Dulbecco's modified Eagle's medium/nutrient mixture F-12 (DMEM/F12) containing 10 % fetal bovine serum (FBS) was used to culture MSCs. For animal experiments, MSCs at passage 4 were suspended in PBS and

infused into NOD mice (5×10^5 cells/mouse) via the tail vein at 13 weeks of age once a week for two consecutive weeks. The mice were sacrificed, and the tissues were collected at 15 weeks of age.

2.5. Histological examination

Murine submandibular glands were fixed in formalin and embedded in paraffin. Five-micrometer sections from the maximum area of the whole submandibular glands were dewaxed using xylene and then dehydrated in a graded series of alcohol for staining with hematoxylin and eosin. Images were captured using a photomicroscope (Olympus, Tokyo, Japan) at $\times 100$ magnification and scored. Histological scores were calculated with the Chisholm-Mason (CM) grade [26]. The average pixels and SEM are displayed graphically.

2.6. Immunohistochemistry

After being deparaffinized and hydrated, submandibular gland sections were heat-treated in citrate buffer (pH 6.0) at 120°C for 15 min. Endogenous peroxidases were blocked with 3 % hydrogen peroxide, followed by overnight incubation with rabbit anti-mouse primary antibodies, including Tim-3 (1:500, Abcam ab241332), E-CAD (1:600, Servicebio GB12082), TGF- $\beta 1$ (1:500, Servicebio GB11179), and α -SMA (1:1000, Servicebio GB111364) at 4°C . Horseradish peroxidase (HRP)-conjugated goat anti-rabbit IgG (1:200, Servicebio GB23303) and horseradish peroxidase (HRP)-conjugated goat anti-mouse IgG (1:200, Servicebio GB23301) were used as the secondary antibodies. The color reaction was performed with freshly prepared 3,3'-diaminobenzidine tetrahydrochloride (DAB) chromogen (Servicebio G1211, Wuhan, China), controlling the development time under microscope observation. Hematoxylin (Servicebio G1004, Wuhan, China) immersion, differentiation liquid (Servicebio G1039, Wuhan, China) differentiation, bluing reagent (Servicebio G1040, Wuhan, China) and neutral gum sealing pieces were used.

2.7. Immunofluorescence

After being deparaffinized and hydrated, submandibular gland sections were heat-treated in antigen repair buffer (pH 8.0) at 120°C for 15 min. After natural cooling, the glass slides were placed in PBS (pH 7.4), shaken, and washed on a decolorization shaking table 3 times for 5 min each time. Endogenous peroxidases were blocked with 3 % hydrogen peroxide, followed by overnight incubation with rabbit anti-mouse primary antibodies, including CD3 (1:1000, Servicebio GB13014), CD8 (1:1000, Servicebio GB13429), and Tim-3 (1:200, Invitrogen 25-5870-82), at 4°C . The slides were washed with PBS (pH 7.4) and incubated for 50 min with horseradish peroxidase (HRP)-conjugated goat anti-rabbit IgG (1:500, Servicebio GB23303). Then, the slides were washed with PBS (pH 7.4) and incubated for 10 min at room temperature with FITC-tyramide (1:1000, Servicebio G1222) and CY3-tyramide (1:1000, Servicebio G1222). The slides were again washed with PBS (pH 7.4), counterstained, and mounted using mounting medium containing 4,6-diamino-2-phenylindole (Servicebio G1012, Wuhan, China). The slides were imaged using laser confocal scanning microscopy (CLSM) (Olympus FV3000, Tokyo, Japan).

2.8. Quantitative real-time polymerase chain reaction

Messenger RNA (mRNA) was extracted using TRIzolTM (InvitrogenTM, 15596018) according to the manufacturer's instructions. Complementary DNA was synthesized using the PrimeScript RT reagent kit (Takara Biotechnology, Tokyo, Japan). QuantStudioTM 6 Flex (Applied Biosystems, Foster City, USA) was used for polymerase chain reaction amplification. All reactions were performed using LightCycler FastStart DNA Master SYBR Green I (Takara Biotechnology, Tokyo, Japan) according to the manufacturer's instructions. All primer sequences were

retrieved from the Origene website (<https://www.origene.com/category/gene-expression/qpcr-primer-pairs>) and verified by blasting them in the NCBI software tool Primer-BLAST (<http://www.ncbi.nlm.nih.gov/tools/primer-blast>). The primers were synthesized by GenScript (Nanjing, China) and are listed in Supplementary Table S1.

2.9. Flow cytometry

Peripheral blood mononuclear cells (PBMCs) were purified from the peripheral blood of SS patients by Ficoll density-gradient centrifugation. Then, PBMCs were incubated with anti-human antibodies to characterize cell subsets: BV510-CD3 (Bio Legend, 317332), APC-CD19 (Invitrogen, 2083510), FITC-CD4 (BD, 550628), PerCP-Cy5.5-CD8 (Bio Legend, 344710), APC-Cy7-L/D (BD, 565388), and SB702-CD366 (Tim-3) (Invitrogen, 67-3109-41). For mice, PBMCs were purified from peripheral blood of NOD and ICR mice by Mouse $1 \times$ Lymphocyte Separation Medium (TBD LTS1092, Tianjin, China). Then, the cells were stained with the following anti-mouse antibodies: BV395-CD3 (BD, 563565), AF700-CD45R (B220) (Invitrogen, 56-0452-82), FITC-CD4 (BD, 553047), BV510-CD8 (Bio Legend, 100752), APC-Cy7-L/D (BD, 565388), and PE-Cy7-CD366 (Tim-3) (Invitrogen, 25-5870-82) for 30 min on ice. The stained cells were assayed by a flow cytometer (BD LSRFortessa), and the data were analysed with FlowJo software.

2.10. In vitro proliferation assay

UC-MSCs (5×10^3) were cultivated in 96-well flat-bottom plates in DMEM/F12 containing 10 % FBS overnight. PBMCs were isolated from the peripheral blood of healthy donors using Ficoll density-gradient centrifugation and then labelled with 10 μM Cell Proliferation Dye eFluorTM 450 (eBioscience, 65-0842-85) in PBS and mixed periodically for 10 min at 37°C . Labelling was quenched by the addition of 4–5 volumes of cold complete media (containing ≥ 10 % FBS) and incubation on ice for 5 min. The labelled cells were then washed twice, counted, and resuspended in Roswell Park Memorial Institute (RPMI) 1640 supplemented with 10 % fetal bovine serum. For some experiments, PBMCs were incubated with a monoclonal Tim-3-blocking antibody (BioLegend, 345009) or IgG1 isotype control (BioLegend, 400165) for 8 h before coculture. The supernatant was removed from the 96-well flat-bottom plates, and 1×10^5 isolated PBMCs were stimulated with 1 $\mu\text{g}/\text{mL}$ anti-CD3 (eBioscience, 16-0037-81) and 1 $\mu\text{g}/\text{mL}$ anti-CD28 (eBioscience, 16-0289-81) antibodies in RPMI 1640 supplemented with 10 % FBS for 3 days. At the end of the culture period, the cells were washed and incubated for 30 min on ice with a combination of the following conjugated anti-human monoclonal antibodies: PE-CF594-CD4 (BioLegend, 317448), PerCP-Cy5.5-CD8 (BD, 560662), and APC-Cy7-L/D (BD, 565388). The stained cells were assayed by a flow cytometer (BD LSRFortessa), and the data were analysed with FlowJo software.

2.11. Statistical analysis

Data are presented as the mean \pm SEM. All statistical analyses were performed using GraphPad Prism 8 software (GraphPad Software, La Jolla, CA, USA). For the normally distributed data, the significance was analysed by Student's *t* tests for two groups or by one-way ANOVA followed by Bonferroni's test for multiple groups. A *P* value < 0.05 was considered significant.

3. Results

3.1. Tim-3 expression level decreases in SS patients

To understand the involvement of Tim-3 in the pathogenesis of SS, we collected peripheral blood mononuclear cells (PBMCs) from pSS patients and healthy controls ($n = 35$ for each group) to measure its

expression by quantitative real-time PCR (qPCR). The results confirmed that the Tim-3 expression level in the PBMCs of pSS patients was significantly lower than that in the PBMCs of healthy controls (Fig. 1A). Furthermore, we recruited eight patients (Table 1) strictly meeting the 2002 American-European Consensus Group (AECG) classification criteria for SS and eight age- and sex-matched healthy volunteers to measure their Tim-3 expression levels in T-cell subsets. Interestingly, our flow cytometry detection demonstrated that the frequencies of Tim-3⁺ subsets in CD3⁺ T cells, CD4⁺ T cells, and CD8⁺ T cells significantly decreased in the SS patients compared with the healthy controls (Fig. 1B). Moreover, among CD3⁺ T, CD4⁺ T, CD8⁺ T, and CD19⁺ B cells, the percentage of CD8⁺ T cells experienced a 50 % increase in the SS patients compared with the healthy controls (Supplementary Fig. S1). Hence, these results indicate the involvement of Tim-3 in SS pathogenesis.

3.2. Tim-3 expression negatively correlates with SS pathogenesis in NOD mice

To further investigate the contribution of Tim-3 to SS, we developed assays using nonobese diabetic (NOD) mice. Flow cytometry analysis of PBMCs indicated the mitigated frequencies of Tim-3⁺ subsets in both CD3⁺ T cells and CD4⁺ T cells in NOD mice in comparison with those in the institute of cancer research (ICR) mice, while there was a downwards trend in cell counts of all these subsets (Fig. 2A). Accordingly, a dramatically higher fraction of CD3⁺ T cells was captured in NOD mice than in ICR mice, and likewise, the percentage of CD4⁺ T cells markedly increased as expected, but the percentage of 45R⁺ B cells unexpectedly decreased (Supplementary Fig. S2). Thus, both CD3⁺ and CD4⁺ T-cell ratios were negatively correlated with the frequencies of their corresponding Tim-3-positive subsets (Supplementary Fig. S2A), similar to the observations in humans. In addition, the detection of Tim-3 expression in PBMCs of NOD mice by qPCR significantly dropped compared with that of ICR mice. (Fig. 2B). Next, we examined the incidence of SS-like symptoms in NOD mice, and our results confirmed an increase in the pathological scores of H&E-stained SMG tissues (Fig. 2C), focal infiltration of inflammatory cells in SMGs (Fig. 2D), and a decrease in the salivary flow rate (Fig. 2E) in NOD mice. Taken together, these results show that the SS-like symptoms in NOD mice derived from focal immune inflammation of exocrine glands are closely related to Tim-3 downregulation in T cells and/or their abnormal proliferation.

3.3. MSC transplantation ameliorates SS symptoms by upregulating Tim-3 in T cells

Considering that umbilical cord (UC)-MSC transplantation effectively suppressed autoimmunity and restored exocrine gland secretory function [27], we designed experiments to determine the roles of Tim-3 in MSC transplantation in NOD mice (Fig. 3A). Strikingly, the frequencies and cell counts of Tim-3⁺CD3⁺ T cells, Tim-3⁺CD4⁺ T cells, and Tim-3⁺CD8⁺ T cells in murine PBMCs considerably increased after MSC transplantation (Fig. 3B). The percentage of CD4⁺ T cells declined by approximately 50 %, while CD8⁺ T cells increased from 22 % to 31 % in the MSC group compared with the PBS group. The percentage of 45R⁺ B cells remained unchanged (Supplementary Fig. S3). The mRNA expression of Tim-3 in the PBMCs of NOD mice was significantly increased after UC-MSC treatment (Fig. 3C). To explain the relationship between the changes in Tim-3 expression in T cells and MSC transplantation-promoted pathological improvement of SS, we examined the therapeutic effects of UC-MSC transplantation on SS in NOD mice. According to the ratings, statistical calculation showed that MSC treatment partially reduced the pathological scores of SMGs (Fig. 3D), which suggests that individual recipients responded differently to MSC transplantation. Pathologically, MSC treatment reduced the scope of lymphocyte infiltration foci or the number of total infiltrating cells, prevented the destruction of glandular duct structure, and alleviated the

damage to glandular epithelial cells (Fig. 3E). Moreover, our results substantiated the negative correlation between the cell counts of Tim-3⁺CD3⁺ T cells and pathological scores of SMGs (Fig. 3F). In contrast to the continuing or even accelerated decline in salivary flow rate in the PBS group, MSC transplantation substantially enabled a slowed decrease of salivary flow rate (Fig. 3G). Altogether, these results indicate that MSC transplantation can elicit a notable immunosuppressive effect by upregulating Tim-3 on excessive T cells, ameliorating the infiltration of target organs, and impairing exocrine function.

3.4. MSC transplantation attenuates Tim-3 expression and alleviates pathological changes in SMGs

To clarify whether Tim-3 participates in the pathological mechanism of SMG in SS, we further examined the expression of Tim-3 in the SMGs of NOD mice. It was noted that Tim-3 showed a significant increase in expression aligning with SS pathogenesis, which nevertheless decreased after MSC treatment in NOD mice (Fig. 4A-B). Concurrently, Gal-9, one of the known ligands of Tim-3, exhibited a similar trend (Fig. 4A), but the other three reported ligands phosphatidylserine (PtdSer) [28], high mobility group box-1 (HMGB1) [29] and carcinoembryonic antigen-related cell adhesion molecule 1 (CEACAM1) [30] did not change (Supplementary Fig. S4A and S4B). Considering the accountability of cytokines and chemokines in the initiation and development of SS [31,32], we then investigated the potential mechanism by which UC-MSC transplantation reduces lymphocyte infiltration in SMGs to alleviate SS (Fig. 4C-F). Intriguingly, our qPCR results showed that the expression of two major SS-associating cytokines, tumor necrosis factor- α (TNF- α) and interferon- γ (IFN- γ), in the SMGs of NOD mice was tremendously downregulated after MSC transplantation and was significantly upregulated in the SS model (Fig. 4C). Further Masson staining solidified the relationship between age and the development of fibrosis in the SMG, which was mitigated by MSC transplantation (Fig. 4D). Then, we analysed the expression of pairs of chemokine (C-X-C motif) ligands (CXCLs)/chemokine (C-X-C motif) receptors (CXCRs). Consistent with previous reports [33,34], we observed the upregulation of CXCL9/CXCL10/CXCR3 and CX3CR1 in the SMGs of 13-week-old NOD mice, suggesting their active involvement in SS pathogenesis. In contrast, the expression levels of all these chemokines and their receptors were diminished in the SMGs after MSC transplantation (Fig. 4E). To distinguish the subsets of infiltrated lymphocytes as well as the expression of Tim-3 in the lymphocyte-infiltrated area of the SMG, we examined the immunofluorescence of SMGs (Fig. 4F). The results revealed CD3⁺ T cells as the major component of focal infiltrating lymphocytes in SMGs, especially with CD8⁺ T cells as a dominant population of infiltrating subsets. In comparison, MSC transplantation hindered the local infiltration of CD3⁺ T cells and CD8⁺ T cells and downregulated Tim-3 expression in the SMG. Thus, our data suggest that MSC transplantation reduced Gal-9/Tim-3 expression, the levels of cytokines and chemokines, and the local infiltration of pathogenic immune cells in the SMG.

3.5. MSC transplantation reverses the EMT of epithelial cells in SMGs and modulates T-cell function via the Gal-9 Tim-3 pathway in vitro

As Tim-3 can promote EMT during tumor cell metastasis, we speculated that it was also involved in EMT-dependent salivary gland fibrosis and chronic inflammatory conditions. We first examined the expression of EMT-related markers in the SMGs of NOD mice (Fig. 5A). The mRNA levels of Vimentin and transforming growth factor beta1 (TGF- β 1) were skyrocketed in the SMGs during the initiation and development of SS but were drastically decreased in the MSC group. Per qPCR results, immunohistochemical identification illustrated that the expression of TGF- β 1 increased in NOD mice from 7 weeks to 13 weeks but declined after MSC transplantation (Fig. 5B).

To explore the molecular mechanism of the Tim-3-involved

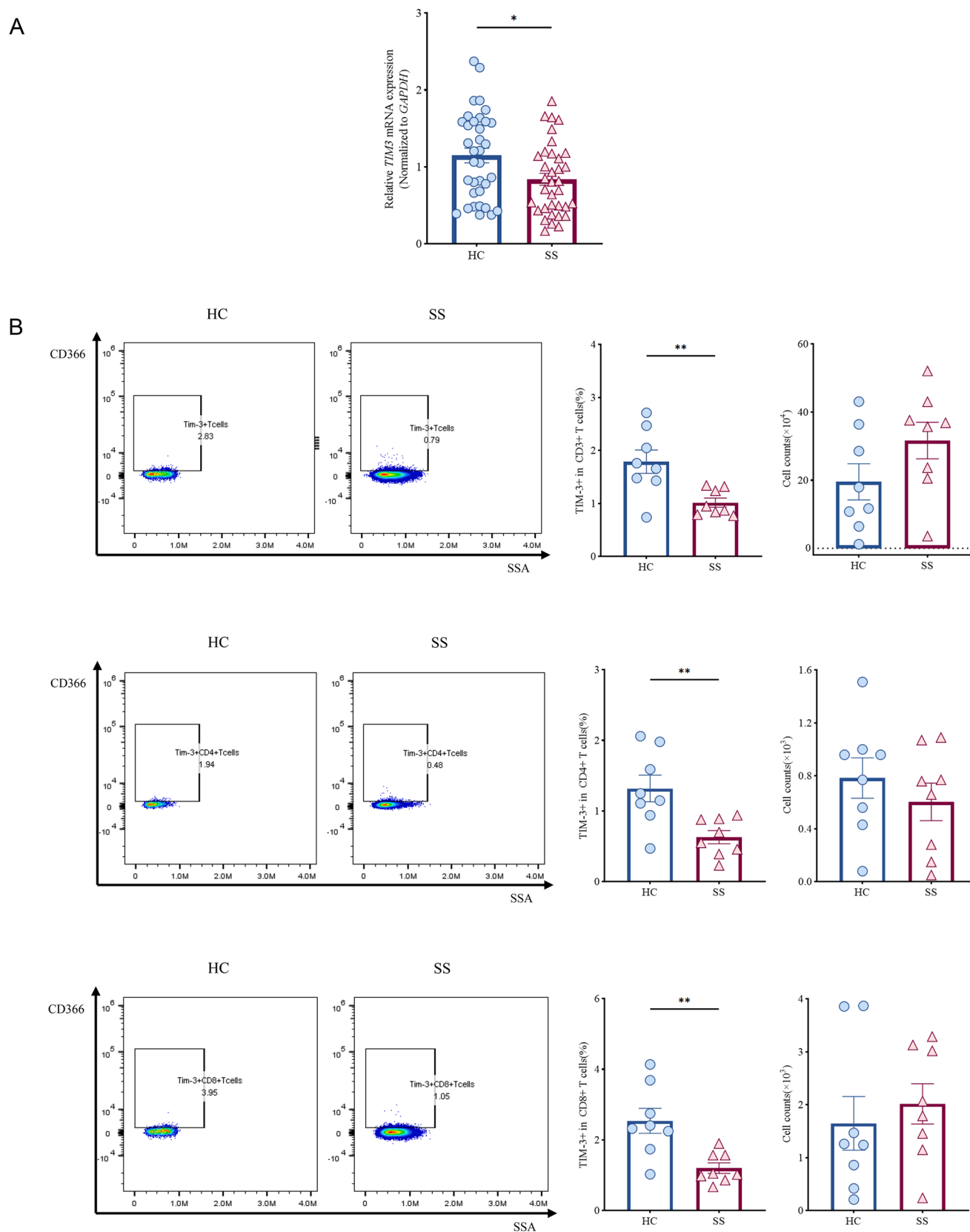


Fig. 1. Tim-3 expression level decreases in SS patients. (A) The mRNA levels of *TIM3* in peripheral blood mononuclear cells from primary Sjögren's syndrome patients ($n = 35$) and healthy controls ($n = 35$) detected by qPCR. (B) Percentage and cell counts of Tim-3⁺ T cells, Tim-3⁺CD4⁺ T cells, and Tim-3⁺CD8⁺ T cells in peripheral blood mononuclear cells from primary Sjögren's syndrome patients ($n = 8$) and healthy controls ($n = 8$) detected by flow cytometry. Data are presented as the mean \pm SEM. *, $p < 0.05$, **, $p < 0.01$.

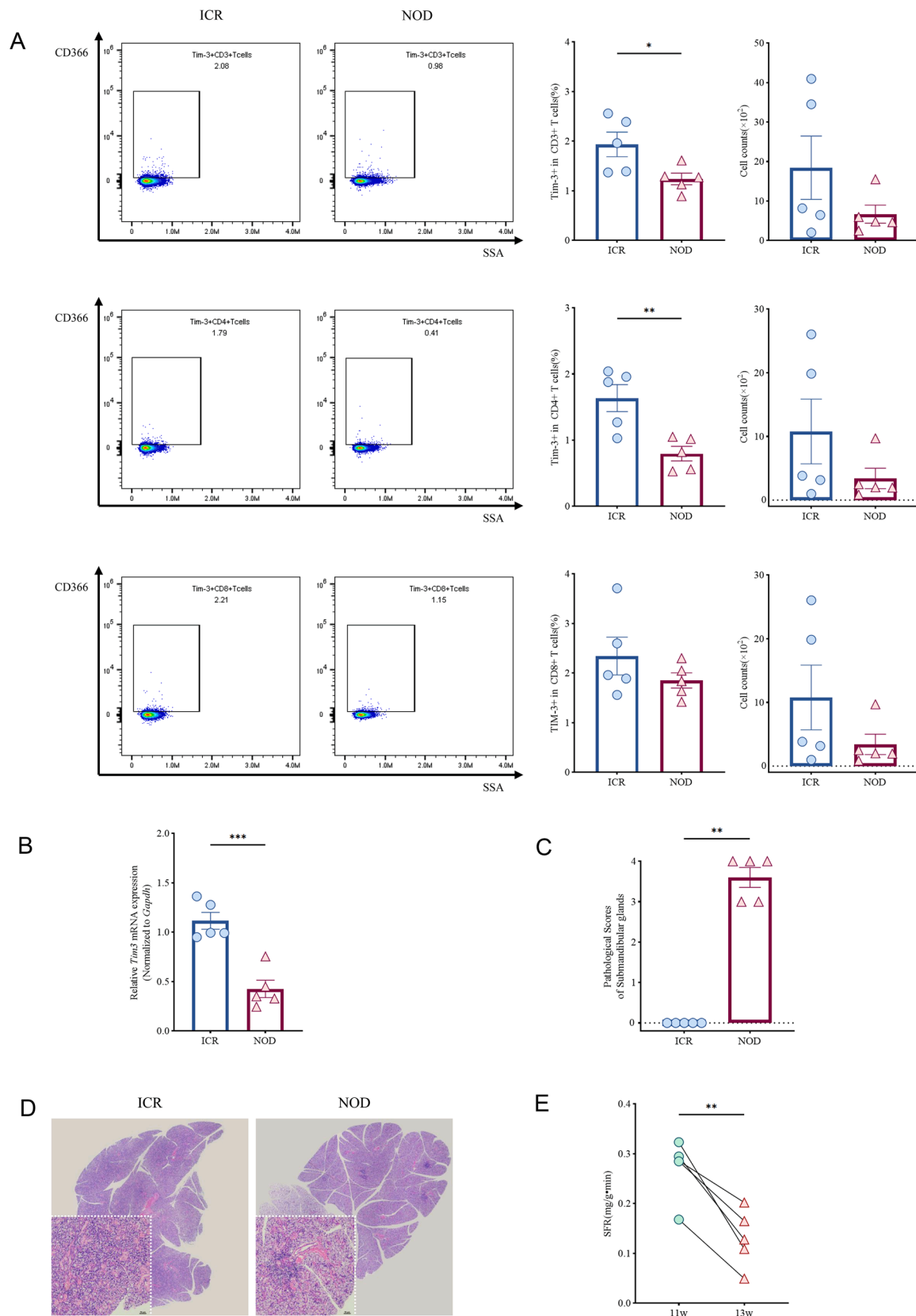


Fig. 2. Tim-3 expression negatively correlates with SS pathogenesis in NOD mice. (A) Percentage and cell counts of Tim-3⁺ T cells, Tim-3⁺CD4⁺ T cells and Tim-3⁺CD8⁺ T cells in PBMCs from ICR (n = 5) (13-week-old) and NOD mice (n = 5) (13-week-old) detected by flow cytometry. (B) The mRNA levels of *Tim3* in PBMCs from ICR (n = 5) (13-week-old) and NOD mice (n = 5) (13-week-old) detected by qPCR. (C) Histopathologic scores for lymphocyte infiltration degree in SMGs from ICR (n = 5) (13-week-old) and NOD mice (n = 5) (13-week-old) based on H&E stained sections of paraffin packed tissues. (D) H&E staining of the SMGs from ICR (n = 5) (13-week-old) and NOD mice (n = 5) (13-week-old). Scale bars, 50 μ m. (E) The salivary flow rate of 11-week-old and 13-week-old NOD mice (n = 5). Data are presented as the mean \pm SEM. *, $p < 0.05$, **, $p < 0.01$, ***, $p < 0.001$.

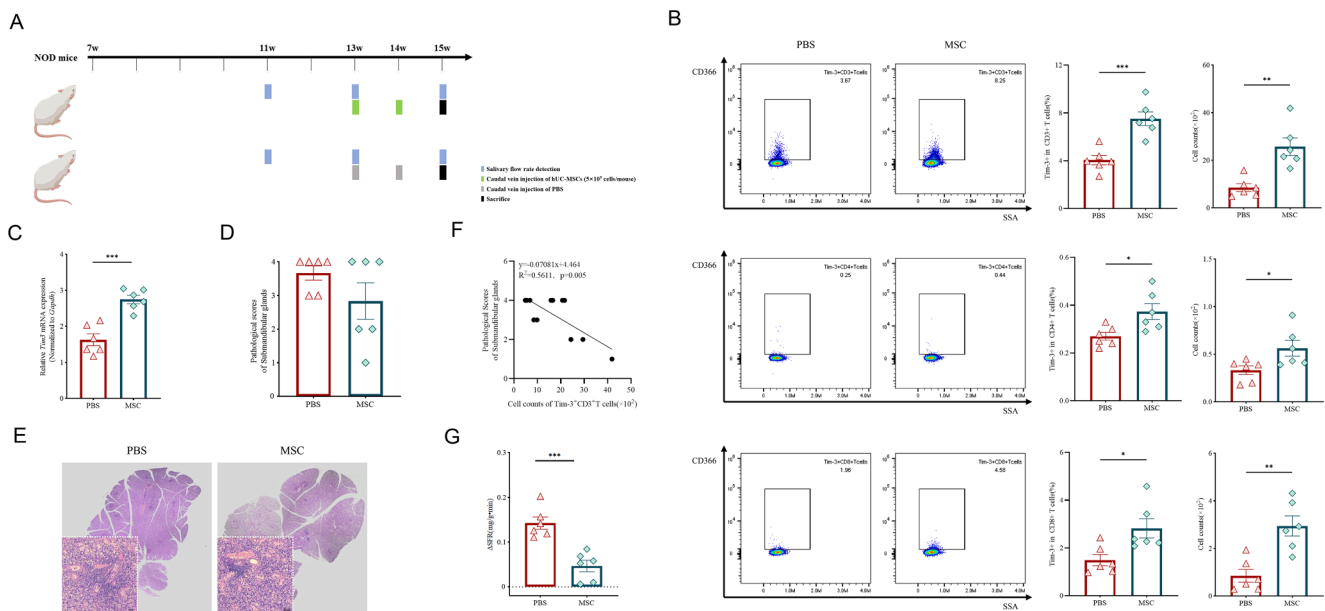


Fig. 3. MSC transplantation ameliorates SS symptoms by upregulating Tim-3 in T cells. (A) An experimental workflow of MSC transplantation in NOD mice. (B) Percentage and cell counts of Tim-3⁺ T cells, Tim-3⁺CD4⁺ T cells and Tim-3⁺CD8⁺ T cells in PBMCs of NOD mice from the PBS (n = 6) (15-week-old) and MSC (n = 6) (15-week-old) treatment groups detected by flow cytometry. (C) The mRNA levels of *Tim3* in peripheral blood mononuclear cells of NOD mice from the PBS (n = 6) (15-week-old) and MSC (n = 6) (15-week-old) treatment groups. (D) Histopathologic scores for the lymphocyte infiltration degree of SMGs of NOD mice from the PBS (n = 6) (15-week-old) and MSC (n = 6) (15-week-old) treatment groups based on H&E-stained sections of paraffin-packed tissues. (E) H&E staining of the SMGs of NOD mice from the PBS (n = 6) (15-week-old) and MSC (n = 6) (15-week-old) treatment groups. Scale bars, 50 μ m. (F) Correlation analysis of Tim-3⁺ T-cell counts in PBMCs and histopathologic scores for the lymphocyte infiltration degree of SMGs (n = 12). (G) The delta salivary flow rate of NOD mice before (13 weeks old) and after (15 weeks old) PBS (n = 6) and MSC (n = 6) treatment. Data are presented as the mean \pm SEM. *, $p < 0.05$, **, $p < 0.01$, ***, $p < 0.001$.

immunosuppressive activity of MSCs, we cocultured human PBMCs with UC-MSCs *in vitro*. Flow cytometry results showed that MSCs exhibited suppressive effects on the proliferation of both whole PBMCs and the CD4⁺/CD8⁺ subsets of PBMCs stimulated by anti-CD3 plus anti-CD28 antibodies (Fig. 5C). However, the immunosuppressive effect of MSCs was abolished by blocking TIM-3 in the whole cells and CD4⁺ subsets but not in the CD8⁺ subsets. Interestingly, the mRNA level of Tim-3 increased in PBMCs cocultured with MSCs (Fig. 5D), but the mRNA level of IFN- γ decreased (Fig. 5E). To understand how MSCs regulate Tim-3 expression, we further examined transcription factors predicted to bind to the *TIM-3* promoter. The results demonstrated that there was significant upregulation of STAT4 and IRF1 as well as downregulation of IFN- γ and T-bet in PBMCs after MSC treatment (Supplementary Fig. S5). These *in vitro* results further prove that Tim-3 plays a vital role in the immunosuppressive function of MSCs.

4. Discussion

MSC transplantation is a powerful approach to treat autoimmune diseases. This study demonstrated that MSC transplantation upregulated the expression of Tim-3 on T cells to inhibit the excessive proliferation of immune cells. Meanwhile the production of proinflammatory factors (TNF α , IFN- γ) and the secretion of chemokines (CX3CL1, CXCL9, CXCL10) were downregulated in the SMG. Through these pathways, MSC transplantation alleviated focal lymphocyte inflammation and improved the exocrine function of NOD mice. Another possible mechanism was that MSCs mitigated fibrosis of the SMG of NOD mice by inhibiting EMT of glandular epithelial cells, which might be a result of downregulation of Tim-3 in the SMG.

As an important CIR, Tim-3 also plays an important role in the pathogenesis of SS, as indicated in this study. Previously, Yang et al. found that the loss of Tim-3 is related to dysregulation of CD4⁺ T-cell function in autoimmune diseases [35]. In our study, the frequencies of Tim-3⁺ subsets in CD4⁺ T cells in NOD mice were significantly decreased compared with those in ICR mice, which could lead to the

excessive proliferation of CD4⁺ T cells. Our results open the exploration of the role of Tim-3 in SS. In the future, it is necessary to perform further experiments to comprehensively identify its expression on various immune cells and explore its regulatory mechanism during the initiation and development of SS.

Mechanistically, Tim-3 seems to serve as an indispensable molecule in MSC treatment for SS based on our results in this study. MSCs inhibit immune cell proliferation by activating the Tim-3 pathway via its ligand Gal-9, which can be strongly induced and secreted from human MSCs upon stimulation with proinflammatory cytokines [21]. Beyond Gal-9, other ligands that have been found to bind to Tim-3 include high mobility group box-1 (HMGB1), carcinoembryonic antigen-related cell adhesion molecule 1 (CEACAM1) and phosphatidylserine (Ptdser). Although we did not find any significant changes in these three ligands at the mRNA level in the SMGs from NOD mice, we still cannot exclude the possible involvement of these ligands in other forms in the therapeutic effect of MSCs. Ptdser is an important marker molecule in apoptosis. Most members of the Tim family have the ability to recognize and bind the metal ion-dependent ligand binding site (MILIBS) of Ptdser but show different functions. Tim-1 mediates T-cell activation, while Tim-3 mediates T-cell elimination [28]. CEACAM1 is an allotopic ligand of Tim-3, which is also expressed on activated T cells and plays a key role in inhibiting T-cell function, determining the tolerance induction function of Tim-3 [30]. The interaction between HMGB1 and Tim-3 was mainly found to reduce the immunogenicity of nucleic acids released by dead tumor cells, representing no predictable connection with autoimmune diseases [29]. However, how MSCs upregulate Tim-3 expression in T cells is still an open question urgent to answer. T-bet, a specific transcription factor of helper T-cell 1 (Th1), was able to upregulate Tim-3 expression in Th1 cells and dendritic cells [36]. Chronic virus infection and continuous antigen stimulation caused increased expression of Tim-3 and PD-1 on CD8⁺ T cells as a result of downregulated T-bet, which eventually led to the severe exhaustion of CD8⁺ T cells [37]. Additionally, both IL-27 and STAT3 have been shown to regulate Tim-3 in tumor-infiltrating lymphocytes [38] and Treg cells

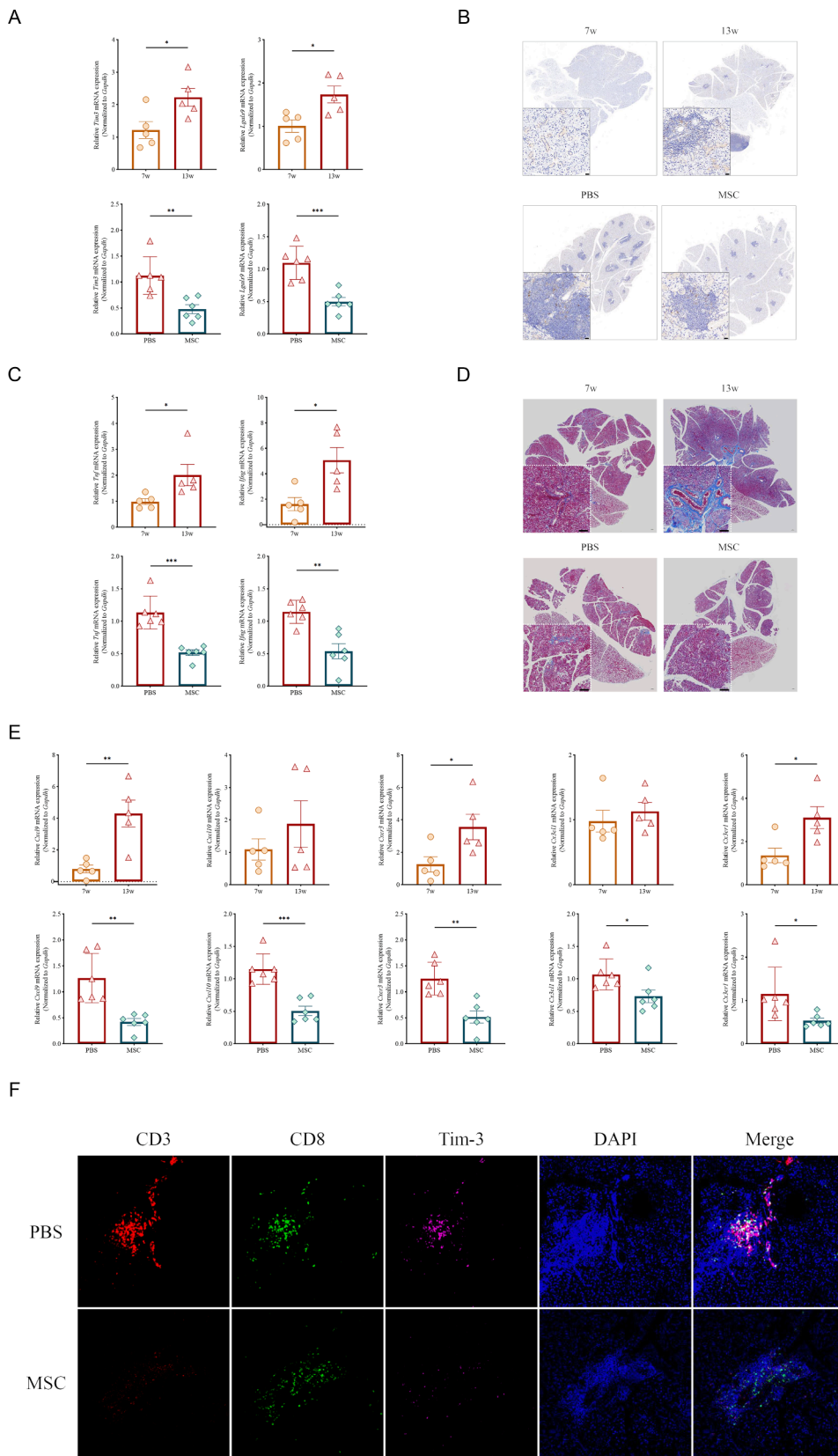


Fig. 4. MSC transplantation attenuates Tim-3 expression and alleviates pathological changes in SMGs. (A) The mRNA levels of *Tim-3* and *Lgals9* in SMGs from 7-week-old NOD mice ($n = 5$) and 13-week-old NOD mice ($n = 5$) compared with NOD mice from PBS ($n = 6$) (15-week-old) and MSC ($n = 6$) (15-week-old) treatment groups. (B) Immunohistochemical staining images of Tim-3 in SMGs from 7-week-old NOD mice ($n = 5$) and 13-week-old NOD mice ($n = 5$) compared with NOD mice from the PBS ($n = 6$) (15-week-old) and MSC ($n = 6$) (15-week-old) treatment groups. Scale bars, 20 μm . (C) The qPCR mRNA levels of *Tnfr* and *Ifng* in SMGs from 7-week-old NOD mice ($n = 5$) and 13-week-old NOD mice ($n = 5$) compared with NOD mice from PBS ($n = 6$) (15-week-old) and MSC ($n = 6$) (15-week-old) treatment groups. (D) Masson's trichrome staining of the SMGs from 7-week-old NOD mice ($n = 5$) and 13-week-old NOD mice ($n = 5$) compared with NOD mice from the PBS ($n = 6$) (15-week-old) and MSC ($n = 6$) (15-week-old) treatment groups. Scale bars, 100 μm . (E) The mRNA levels of *Cxcl9/Cxcl10/Cxcr3* and *Cx3cl1/Cx3cr1* in SMGs from ICR ($n = 5$) (13-week-old) and NOD mice ($n = 5$) (13-week-old) compared with NOD mice from PBS ($n = 6$) (15-week-old) and MSC ($n = 6$) (15-week-old) treatment groups. (F) Representative fluorescence microphotographs of SMGs from NOD mice from the PBS ($n = 6$) (15 weeks old) and MSC ($n = 6$) (15 weeks old) treatment groups. Immunostained for CD3 (red), CD8 (green), Tim-3 (pink) and counterstained with 4',6-diamidino-2-phenylindole (DAPI; blue) for nuclei. Scale bars, 50 μm . Data are presented as the mean \pm SEM. *, $p < 0.05$, **, $p < 0.01$, ***, $p < 0.001$.

[39]. Notably, in this work, we only detected significant upregulation of STAT4 and IRF1 with downregulation of IFN- γ and T-bet, implying that these transcription factors are likely important transcription factors that promote Tim-3 expression in T cells after MSC treatment. It is also

interesting to further clarify the beneficial effects of MSC treatment for SS mainly through Tim-3 modulation in which specific T cells are present.

Apart from Tim-3, MSC transplantation resulted in a decrease in the

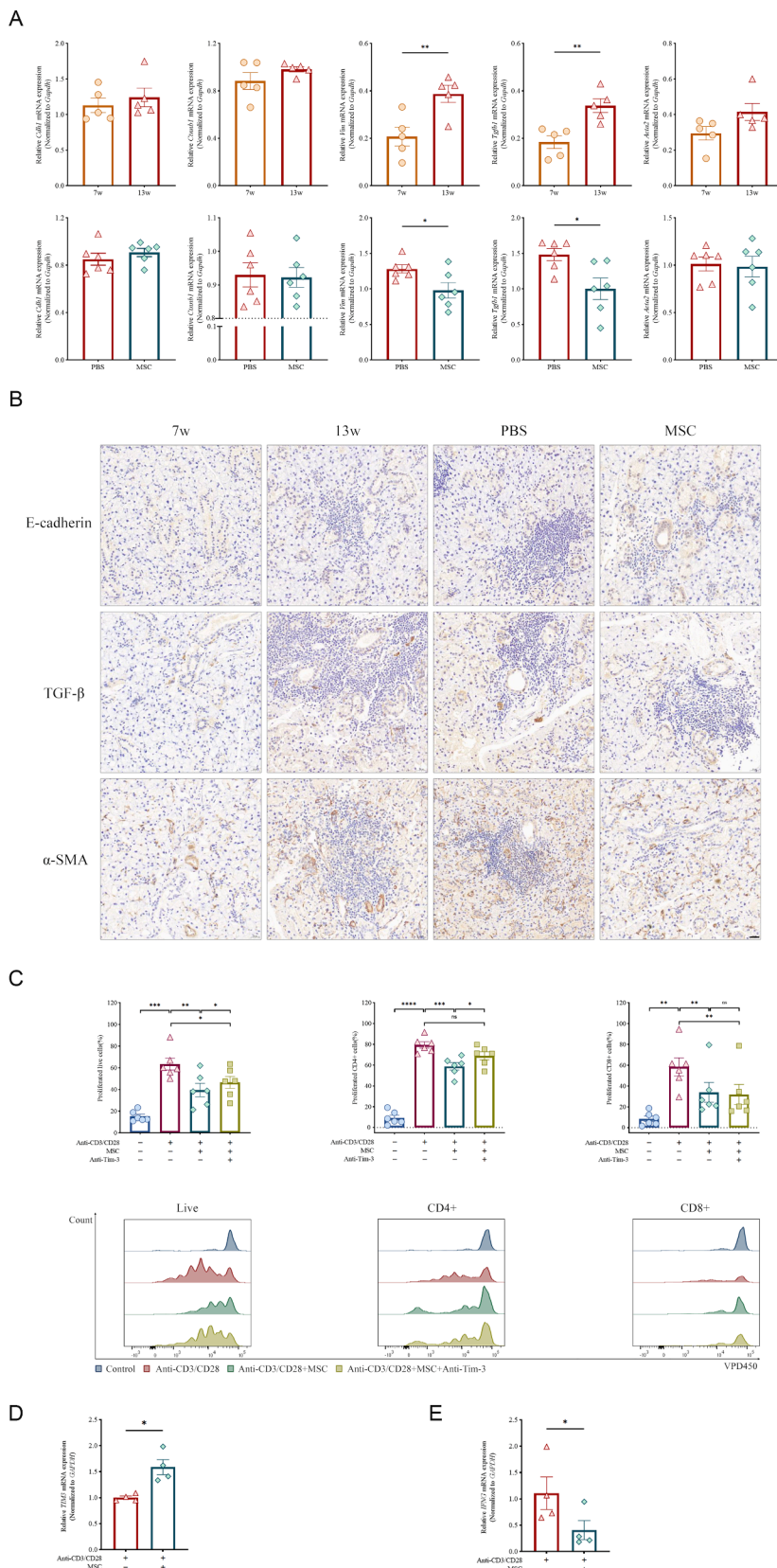


Fig. 5. MSC transplantation reverses the EMT of epithelial cells in SMG and modulates T-cell function via the Gal-9/Tim-3 pathway *in vitro*. (A) The mRNA levels of EMT-related genes in SMGs from NOD mice (7 weeks old; 13 weeks old) compared with NOD mice from the PBS (15 weeks old) and MSC (15 weeks old) treatment groups. (B) Immunohistochemical staining for the EMT-related markers TGF- β , α -SMA, and E-cadherin in the SMGs from NOD mice (7 weeks old; 13 weeks old) compared with NOD mice from the PBS (15 weeks old) and MSC (15 weeks old) treatment groups. (C) Cell proliferation of PBMCs from healthy donors was detected using VPD450 staining. Proliferative percentages were calculated. Histogram half overlays of proliferation in whole live PBMCs, CD4⁺ cells, and CD8⁺ cells are shown. *In vitro* experiments consisted of four subgroups oriented to different culture conditions: without stimulation, stimulated with anti-CD3/CD28, stimulated with anti-CD3/CD28, cocultured with MSCs, stimulated with anti-CD3/CD28, pretreated with anti-Tim-3 antibodies, and then cocultured with MSCs. Data are presented as the mean \pm SEM. *, $p < 0.05$, **, $p < 0.01$, ***, $p < 0.001$, ****, $p < 0.0001$.

inflammatory factors TNF- α and IFN- γ in the SMG. Such anti-inflammatory effects of MSCs are consistent with a previous study on MSC exosomes [40]. MSC transplantation also reversed the EMT of glandular epithelial cells via downregulation of Tim-3 in the SMG.

Similar reversal progress induced by MSCs was observed through inhibiting the NF- κ B pathway [41]. Tim-3 has been identified as a promoter of tumor metastasis by inducing EMT via the SNAIL1 pathway [19]. Notably, we have identified that the expression level of Tim-3 in

the SMG increased after MSC transplantation. IHC-positive staining of Tim-3 was observed in both glandular epithelial cells and lymphocytes in the SMG, but the strongly stained cells were mainly enriched in lymphocytes. As a result, the overall expression of Tim-3 consists of the quantity of infiltrated lymphocytes in the SMG. While MSC transplantation reduced lymphocyte infiltration in the SMG, downregulated Tim-3 further reduced the destruction of the SMG by inhibiting EMT. In a sense, Tim-3 and MSC may be mutually causal and interact through the binding between Tim-3 and Gal-9.

5. Conclusion

Taken together, we have revealed a new mechanism of MSC treatment in immunity re-equilibrium mediated by the upregulation of Tim-3 expression on overactivated T cells and restoration of morphology and function of the submandibular gland through inhibiting inflammation, lymphocyte infiltration, fibrosis, and EMT induced by downregulated Tim-3. We attempt to gather all these abovementioned results in a schematic illustration (Supplementary Fig. S6). However, we did not extend the study of Tim-3 to other immune cells to outline the panorama of the effect of Tim-3 on the whole immune system. In addition, more studies are required to elucidate the specific mechanism by which Tim-3 inhibits immune cell proliferation and regulates EMT.

CRediT authorship contribution statement

Tian Sun: Investigation, Formal analysis, Visualization, Methodology, Data curation, Writing – original draft, Resources, Writing – review & editing. **Shanshan Liu:** Investigation, Resources. **Guangxia Yang:** Conceptualization, Methodology, Data curation. **Rujie Zhu:** Investigation, Resources. **Zutong Li:** Resources, Formal analysis, Data curation. **Genhong Yao:** Methodology, Funding acquisition. **Hongwei Chen:** Methodology, Validation, Data curation, Writing – review & editing, Supervision. **Lingyun Sun:** Supervision, Writing – review & editing, Project administration, Funding acquisition, Conceptualization, Methodology, Writing – review & editing, Project administration, Funding acquisition.

Declaration of Competing Interest

The authors declare that they have no known competing financial interests or personal relationships that could have appeared to influence the work reported in this paper.

Data availability

No data was used for the research described in the article.

Acknowledgements

This study was supported by the National Key R&D Program of China (2020YFA0710800), the Major International Regional Joint Research Project of China (81720108020), the Key Project supported by the Medical Science and Technology Development Foundation, Nanjing Department of Health (ZKX20019), and Natural Science Foundation of China (NSFC) (81970062 and 81770061).

Appendix A. Supplementary material

Supplementary data to this article can be found online at <https://doi.org/10.1016/j.intimp.2022.109152>.

References

- [1] G.E. Ehrlich, Kelley's textbook of rheumatology, JAMA 302 (2009) 900–904, <https://doi.org/10.1001/jama.2009.1254>.
- [2] B. Qin, et al., Epidemiology of primary Sjogren's syndrome: a systematic review and meta-analysis, Ann. Rheum. Dis. 74 (2015) 1983–1989, <https://doi.org/10.1136/annrheumdis-2014-205375>.
- [3] C. Chivasso, J. Sarraud, J. Perret, C. Delporte, M.S. Soyfoo, The involvement of innate and adaptive immunity in the initiation and perpetuation of Sjogren's syndrome, Int. J. Mol. Sci. 22 (2021), <https://doi.org/10.3390/ijms22020658>.
- [4] M.R. Hillen, F.A. Ververs, A.A. Kruijs, J.A. Van Roon, Dendritic cells, T-cells and epithelial cells: a crucial interplay in immunopathology of primary Sjogren's syndrome, Expert Rev. Clin. Immunol. 10 (2014) 521–531, <https://doi.org/10.1586/1744666X.2014.878650>.
- [5] N. Li, J. Hua, Interactions between mesenchymal stem cells and the immune system, Cell Mol. Life Sci. 74 (2017) 2345–2360, <https://doi.org/10.1007/s00018-017-2473-5>.
- [6] J. Qi, X. Tang, W. Li, W. Chen, G. Yao, L. Sun, Mesenchymal stem cells inhibited the differentiation of MDSCs via COX2/PGE2 in experimental sialadenitis, Stem Cell Res. Ther. 11 (1) (2020), <https://doi.org/10.1186/s13287-020-01837-x>.
- [7] T. Zhou, Z. Yuan, J. Weng, D. Pei, X. Du, C. He, P. Lai, Challenges and advances in clinical applications of mesenchymal stromal cells, J. Hematol. Oncol. 14 (1) (2021), <https://doi.org/10.1186/s13045-021-01037-x>.
- [8] M. Matsumura-Kawashima, et al., Secreted factors from dental pulp stem cells improve Sjogren's syndrome via regulatory T cell-mediated immunosuppression, Stem Cell Res. Ther. 12 (2021) 182, <https://doi.org/10.1186/s13287-021-02236-6>.
- [9] J. Xu, et al., Allogeneic mesenchymal stem cell treatment alleviates experimental and clinical Sjogren syndrome, Blood 120 (2012) 3142–3151, <https://doi.org/10.1182/blood-2011-11-391144>.
- [10] T. Comont, et al., Immune-related adverse events after immune checkpoints inhibitors in 2019: an update, Rev. Med. Interne 41 (2020) 37–45, <https://doi.org/10.1016/j.revmed.2019.09.005>.
- [11] M.A. Couey, R.B. Bell, A.A. Patel, M.C. Romba, M.R. Crittenden, B.D. Curti, W. J. Urb, R.S. Leidner, Delayed immune-related events (DIRE) after discontinuation of immunotherapy: diagnostic hazard of autoimmunity at a distance, J. Immunother. Cancer 7 (1) (2019), <https://doi.org/10.1186/s40425-019-0645-6>.
- [12] G. Thompson, A. McLean-Tooke, J. Wrobel, M. Lavender, M. Lucas, Sjogren syndrome with associated lymphocytic interstitial pneumonia successfully treated with tacrolimus and abatacept as an alternative to rituximab, Chest 153 (2018) e41–e43, <https://doi.org/10.1016/j.chest.2017.12.010>.
- [13] Y. Cao, et al., Role of Tim-3 in regulating tumorigenesis, inflammation, and antitumor immunity therapy, Cancer Biomark 32 (2021) 237–248, <https://doi.org/10.3233/CBM-210114>.
- [14] C. Zhu, A.C. Anderson, A. Schubart, H. Xiong, J. Imitola, S.J. Khoury, X.X. Zheng, T.B. Strom, V.K. Kuchroo, The Tim-3 ligand galectin-9 negatively regulates T helper type 1 immunity, Nat. Immunol. 6 (12) (2005) 1245–1252.
- [15] T. Asano, N. Matsuo, Y. Fujita, H. Matsumoto, J. Temmoku, M. Yashiro-Furuya, S. Sato, E. Suzuki, H. Kobayashi, H. Watanabe, K. Migita, Serum levels of T cell immunoglobulin and mucin-domain containing molecule 3 in patients with systemic lupus erythematosus, J. Clin. Med. 9 (11) (2020) 3563.
- [16] M. Nakazawa, K. Suzuki, M. Takeshita, J. Inamo, H. Kamata, M. Ishii, Y. Oyamada, H. Oshima, T. Takeuchi, Distinct expression of coinhibitory molecules on alveolar T cells in patients with rheumatoid arthritis-associated and idiopathic inflammatory myopathy-associated interstitial lung disease, Arthritis Rheumatol. 73 (4) (2021) 576–586.
- [17] R. Liberal, C.R. Grant, B.S. Holder, Y. Ma, G. Mieli-Vergani, D. Vergani, M. S. Longhi, The impaired immune regulation of autoimmune hepatitis is linked to a defective galectin-9/tim-3 pathway, Hepatology 56 (2) (2012) 677–686.
- [18] H. Matsumoto, Y. Fujita, N. Matsuo, J. Temmoku, M. Yashiro-Furuya, T. Asano, S. Sato, H. Watanabe, E. Suzuki, S. Tsuji, S. Fukui, M. Umeda, N. Iwamoto, A. Kawakami, K. Migita, Serum checkpoint molecules in patients with IgG4-related disease (IgG4-RD), Arthritis Res. Ther. 23 (1) (2021), <https://doi.org/10.1186/s13075-021-02527-6>.
- [19] Y. Xiao, et al., TIM-3 participates in the invasion and metastasis of nasopharyngeal carcinoma via SMAD7/SMAD2/SMAD1 axis-mediated epithelial-mesenchymal transition, Onco. Targets Ther. 13 (2020) 1993–2006, <https://doi.org/10.2147/OTT.S237222>.
- [20] M. Sisto, et al., Interleukin-17 and -22 synergy linking inflammation and EMT-dependent fibrosis in Sjogren's syndrome, Clin. Exp. Immunol. 198 (2019) 261–272, <https://doi.org/10.1111/cei.13337>.
- [21] S.N. Kim, H.J. Lee, M.S. Jeon, T. Yi, S.U. Song, Galectin-9 is involved in immunosuppression mediated by human bone marrow-derived clonal mesenchymal stem cells, Immune Netw. 15 (2015) 241–251, <https://doi.org/10.4110/in.2015.15.5.241>.
- [22] A.B. Peck, C.Q. Nguyen, What can Sjogren's syndrome-like disease in mice contribute to human Sjogren's syndrome? Clin. Immunol. 182 (2017) 14–23, <https://doi.org/10.1016/j.clim.2017.05.001>.
- [23] J.E. Craighead, Experimental models of juvenile onset (insulin-dependent) diabetes mellitus, Monogr. Pathol. 21 (1980) 166–176.
- [24] D.S. Kim, et al., Short-chain fatty acid butyrate induces IL-10-producing B cells by regulating circadian-clock-related genes to ameliorate Sjogren's syndrome, J. Autoimmun. 119 (2021), 102611, <https://doi.org/10.1016/j.jaut.2021.102611>.
- [25] D. Wang, X. Feng, L. Lu, J.E. Konkel, H. Zhang, Z. Chen, X. Li, X. Gao, L. Lu, S. Shi, W. Chen, L. Sun, A CD8 T cell/indoleamine 2,3-dioxygenase axis is required for mesenchymal stem cell suppression of human systemic lupus erythematosus, Arthritis Rheumatol. 66 (8) (2014) 2234–2245.
- [26] D.M. Chisholm, D.K. Mason, Labial salivary gland biopsy in Sjogren's disease, J. Clin. Pathol. 21 (1968) 656–660, <https://doi.org/10.1136/jcp.21.5.656>.

- [27] R. Liu, et al., Umbilical cord mesenchymal stem cells inhibit the differentiation of circulating T follicular helper cells in patients with primary Sjogren's syndrome through the secretion of indoleamine 2,3-dioxygenase, *Rheumatology (Oxford)* 54 (2015) 332–342, <https://doi.org/10.1093/rheumatology/keu316>.
- [28] R.H. DeKruyff, X. Bu, A. Ballesteros, C. Santiago, Y.-L. Chim, H.-H. Lee, P. Karisola, M. Pichavant, G.G. Kaplan, D.T. Umetsu, G.J. Freeman, J.M. Casasnovas, T cell/ transmembrane, Ig, and mucin-3 allelic variants differentially recognize phosphatidylserine and mediate phagocytosis of apoptotic cells, *J. Immunol.* 184 (4) (2010) 1918–1930.
- [29] S. Chiba, M. Baghdadi, H. Akiba, H. Yoshiyama, I. Kinoshita, H. Dosaka-Akita, Y. Fujioka, Y. Ohba, J.V. Gorman, J.D. Colgan, M. Hirashima, T. Uede, A. Takaoka, H. Yagita, M. Jinushi, Tumor-infiltrating DCs suppress nucleic acid-mediated innate immune responses through interactions between the receptor TIM-3 and the alarmin HMGB1, *Nat. Immunol.* 13 (9) (2012) 832–842.
- [30] Y.-H. Huang, C. Zhu, Y. Kondo, A.C. Anderson, A. Gandhi, A. Russell, S.K. Dougan, B.-S. Petersen, E. Melum, T. Pertel, K.L. Clayton, M. Raab, Q. Chen, N. Beauchemin, P.J. Yazaki, M. Pyzik, M.A. Ostrowski, J.N. Glickman, C.E. Rudd, H.L. Ploegh, A. Franke, G.A. Petsko, V.K. Kuchroo, R.S. Blumberg, CEACAM1 regulates TIM-3-mediated tolerance and exhaustion, *Nature* 517 (7534) (2015) 386–390.
- [31] R. Fernandez-Ruiz, T.B. Niewold, Type I interferons in autoimmunity, *J. Invest. Dermatol.* 142 (3) (2022) 793–803.
- [32] S.L. Carter, M. Muller, P.M. Manders, I.L. Campbell, Induction of the genes for Cxcl9 and Cxcl10 is dependent on IFN-gamma but shows differential cellular expression in experimental autoimmune encephalomyelitis and by astrocytes and microglia in vitro, *Glia* 55 (2007) 1728–1739, <https://doi.org/10.1002/glia.20587>.
- [33] N. Ogawa, L. Ping, L. Zhenjun, Y. Takada, S. Sugai, Involvement of the interferon-gamma-induced T cell-attracting chemokines, interferon-gamma-inducible 10-kd protein (CXCL10) and monokine induced by interferon-gamma (CXCL9), in the salivary gland lesions of patients with Sjogren's syndrome, *Arthritis Rheum.* 46 (2002) 2730–2741, <https://doi.org/10.1002/art.10577>.
- [34] E. Astorri, R. Scrivo, M. Bombardieri, G. Picarelli, I. Pecorella, A. Porzia, G. Valesini, R. Priori, CX3CL1 and CX3CR1 expression in tertiary lymphoid structures in salivary gland infiltrates: fractalkine contribution to lymphoid neogenesis in Sjogren's syndrome, *Rheumatology (Oxford)* 53 (4) (2014) 611–620.
- [35] L. Yang, D.E. Anderson, J. Kuchroo, D.A. Hafler, Lack of TIM-3 immunoregulation in multiple sclerosis, *J. Immunol.* 180 (2008) 4409–4414, <https://doi.org/10.4049/jimmunol.180.7.4409>.
- [36] A.C. Anderson, G.M. Lord, V. Dardalhon, D.H. Lee, C.A. Sabatos-Peyton, L. H. Glimcher, V.K. Kuchroo, T-bet, a Th1 transcription factor regulates the expression of Tim-3, *Eur. J. Immunol.* 40 (3) (2010) 859–866.
- [37] C. Kao, K.J. Oestreich, M.A. Paley, A. Crawford, J.M. Angelosanto, M.-A. Ali, A. M. Intlekofer, J.M. Boss, S.L. Reiner, A.S. Weinmann, E.J. Wherry, Transcription factor T-bet represses expression of the inhibitory receptor PD-1 and sustains virus-specific CD8+ T cell responses during chronic infection, *Nat. Immunol.* 12 (7) (2011) 663–671.
- [38] C. Zhu, K. Sakuishi, S. Xiao, Z. Sun, S. Zaghouani, G. Gu, C. Wang, D.J. Tan, C. Wu, M. Rangachari, T. Pertel, H.-T. Jin, R. Ahmed, A.C. Anderson, V.K. Kuchroo, An IL-27/NFIL3 signalling axis drives Tim-3 and IL-10 expression and T-cell dysfunction, *Nat. Commun.* 6 (1) (2015), <https://doi.org/10.1038/ncomms7072>.
- [39] L. Huang, Y. Xu, J. Fang, W. Liu, J. Chen, Z. Liu, Q. Xu, Targeting STAT3 abrogates Tim-3 upregulation of adaptive resistance to PD-1 blockade on regulatory T cells of melanoma, *Front. Immunol.* 12 (2021), 654749, <https://doi.org/10.3389/fimmu.2021.654749>.
- [40] L. Guo, et al., Extracellular vesicles from mesenchymal stem cells prevent contact hypersensitivity through the suppression of Tc1 and Th1 cells and expansion of regulatory T cells, *Int. Immunopharmacol.* 74 (2019), 105663, <https://doi.org/10.1016/j.intimp.2019.05.048>.
- [41] K. Xiao, et al., Mesenchymal stem cells reverse EMT process through blocking the activation of NF-kappaB and Hedgehog pathways in LPS-induced acute lung injury, *Cell Death Dis* 11 (2020) 863, <https://doi.org/10.1038/s41419-020-03034-3>.